FLORY, P. J. (1962). *J. Am. Chem. Soc.* **84**, 2857–2867.
FUJIWARA, Y. & FLORY, P. J. (1970). *Macromolecules*, **3**, 288–293.
KING, J. S., SUMMERFIELD, G. C., BAI, S. J., TENG, W. H., HIGGINS, J. S. & ULLMAN, R. (1978). To be published.
MANDELKERN, L. (1970). *Prog. Polym. Sci.* **2**, 165–200.
MANDELKERN, L. (1976). *Acc. Chem. Res.* **9**, 81–86.
SADLER, D. M. & KELLER, A. (1976). *Polymer*, **17**, 37–40.
SADLER, D. M. & KELLER, A. (1977). *Macromolecules*, **10**, 1128–1140.
SCHELTEN, J., BALLARD, D. G. H. & WIGNALL, G. D. (1978). To be published.
SCHELTEN, J., BALLARD, D. G. H., WIGNALL, G. D., LONGMAN, G. W. & SCHMATZ, W. (1976). *Polymer*, **17**, 751–757.
YOON, D. Y. & FLORY, P. J. (1975). *Polymer*, **16**, 645–648.
YOON, D. Y. & FLORY, P. J. (1977). *Polymer*, **18**, 509–513.

J. Appl. Cryst. (1978). **11**, 535–539

Determination of the Interface Distribution Function of Lamellar Two-Phase Systems

By N. STRIBECK and W. RULAND, *Universität Marburg, Fachbereich Physikalische Chemie, Bereich Polymere, D-3550 Marburg/Lahn, Lahnberge, Gebäude H, Federal Republic of Germany*

(*Received* 7 *January* 1978; *accepted* 4 *May* 1978)

The concept of interface distribution functions [Ruland (1977), *Colloid Polym. Sci.* **255**, 417–427] has been applied to the evaluation of the small-angle scattering of a series of polyethylene samples. The results indicate that the statistics of the lamellar stacking is not necessarily determined by next-neighbor interactions and that non-negligible volume fractions of amorphous domains outside the lamellar systems are observed in a number of samples.

1. Introduction

Lamellar two-phase superstructures occur very frequently in polymers, and X-ray small-angle scattering is widely used for the study of these structures. In many cases the evaluation of the scattering curves has been restricted to the determination of the Bragg spacing from the interference maxima, which is a measure of the average repeat distance of the lamellar stacking called 'long period'. More involved methods (Tsvankin, Zubov & Kitaigorodskii, 1968; Strobl & Müller, 1973; Brämer, 1974; Kilian & Wenig, 1974) use further details of the scattering curve (*e.g.* line width, intensity distribution) to obtain supplementary information.

Most of these methods are based on structural models with a limited number of parameters; hence the significance of the results depends strongly on the applicability of these models.

The fewest *a priori* assumptions are made in the determination of the one-dimensional correlation function (Vonk & Kortleve, 1967). This correlation function is, however, relatively insensitive to structural details. It was shown in a recent paper (Ruland, 1977) that more structural details can be resolved in the interface distribution function which is obtained by Fourier transformation of suitably corrected experimental intensity curves.

In the present paper, this method has been applied to small-angle scattering curves of polyethylene samples of various crystallinities in order to check its applicability and limits.

2. Theoretical

A detailed discussion of the theoretical basis for the determination of interface distribution functions is given in the earlier paper (Ruland, 1977). For the purpose of this paper it is thus sufficient to present a summary of the basic equations.

Let us first consider scattering curves measured with pinhole collimation. The scattering intensity I_{obs} is determined over a wide enough range so that the intensity component I_{Fl} due to density fluctuations within the phases can be determined by extrapolation from the wide-angle region where I_{Fl} is predominant. This extrapolation can be facilitated by $\log I$ *vs* s^2 plots (Rathje & Ruland, 1976). The difference $I_{obs}-I_{Fl}$ is then multiplied by s^4, where $s=2\sin\theta/\lambda$ is the distance in reciprocal space, and plotted against s^2 in order to determine the width of the domain boundary d_z. Knowing d_z one can correct the scattering intensity for the finite width of the domain boundary. The result is I_{id}, the scattering intensity of a lamellar two-phase system with infinitely sharp domain boundaries. This intensity distribution should follow Porod's law for large values of s. From the difference between I_{id} and its asymptote at large values of s one obtains the interference function $G_1(s)$

$$\frac{1}{t}G_1(s)=\frac{8\pi^3}{V}\left[\lim_{s\to\infty} s^4 I_{id}-s^4 I_{id}\right], \qquad (1)$$

where t is the thickness of and V the volume occupied by the stacks of lamellae.

The interface distribution function $g_1(r)$ is then obtained by a Fourier cosine transform of $G_1(s)$:

$$g_1(r)=2\int_0^\infty G_1(s)\cos 2\pi rs\,ds\,. \qquad (2)$$

In the case of scattering curves measured with slit collimation, the procedure for correcting the observed intensity J_{obs} is similar to that for I_{obs}. From the difference $J_{obs}-J_{Fl}$ multiplied by s^3 one determines d_z and thus J_{id}. From this

the interference function $\tilde{G}_1(s)$ is obtained as

$$\frac{1}{t}\tilde{G}_1(s)=\frac{16\pi^2}{V}[\lim_{s\to\infty} s^3 J_{id}(s)-s^3 J_{id}]. \quad (3)$$

In contrast to equation (2), the relationship between $\tilde{G}_1(s)$ and $g_1(r)$ is given by a more complicated integral transform with Bessel functions of orders zero to three as kernel,

$$g_1(r)=\int_0^\infty \tilde{G}_1(s)K(rs)\mathrm{d}s, \quad (4)$$

where

$$K(rs)=\frac{\pi}{4}(3[J_0(2\pi rs)-J_2(2\pi rs)] + \pi rs[J_3(2\pi rs)-J_1(2\pi rs)]).$$

The angular region in J in which Porod's law is valid may be outside the validity of the approximation of 'infinite' slit height. In this case, the determination of d_z and J_{id} can be carried out by a method described in an earlier paper (Ruland, 1974) in which the profile of the slit is approximated by a trapezoid.

In order to study the effect of the statistics of the lamellar stacking and the stack size on the interface distribution functions we have computed $g_1(r)$ functions for various types of stacking models assuming Gaussian distributions to represent the variation of interface distances. In this case, $g_1(r)$ is given by

$$g_1(r)=\sum_{i=1}^{\infty} w_i h_i(r-r_i), \quad (5)$$

where w_i are the weights of the Gaussian distance distributions h_i which are centered on r_i. If we consider normalized distributions,

$$\int_{-\infty}^{\infty} h_i(r)\mathrm{d}r=1,$$

h_i is given by

$$h_i=\frac{1}{\sigma_i\sqrt{2\pi}}\exp\left(-\frac{r^2}{2\sigma_i^2}\right),$$

where σ_i is the r.m.s. variation of the ith distance distribution. For the types of stacking distributions we are interested in, the most convenient indexing is $i=1$ for the spacings between adjacent interfaces corresponding to the thicknesses of the lamellae of the phase with the lower volume concentration, $i=2$ for the spacings between adjacent interfaces corresponding to the thicknesses of the lamellae of the phase with the higher volume concentration, $i=3$ for the distances to the second next interface, $i=4$ for the distance to the third next interface containing the thicknesses of two lamellae of the phase with the lower volume concentration and one lamella of the phase of higher volume concentration, *etc.* The correspondence to the more general notation used in the earlier paper (Ruland, 1977) is given in Table 1.

Table 1. *Correspondence of general and simplified index for distance distributions*

General	Simplified
1	1
2	2
12,21	3
121	4
212	5
1212,2121	6
12121	7
21212	8

The conversion is thus

$$i=n_1+2n_2,$$

where n_1 and n_2 are the multiplicities with which the indices 1 and 2, respectively, occur in the general index. With this notation, the r_i values are given by

$$r_i=n(r_1+r_2) \quad \text{for} \quad i=3n,$$
$$r_i=n(r_1+r_2)+r_1 \quad \text{for} \quad i=3n+1,$$
$$r_i=n(r_1+r_2)+r_2 \quad \text{for} \quad i=3n+2.$$

For an infinite stack size, the weight functions are

$$w_i=1 \quad \text{for} \quad i\neq 3n,$$
$$w_i=-2 \quad \text{for} \quad i=3n$$

and a first approximation for finite stack sizes is given by

$$w_i=\exp(-r_i/t) \quad \text{for} \quad i\neq 3n,$$
$$w_i=-2\exp(-r_i/t) \quad \text{for} \quad i=3n,$$

where t is the average thickness of the stack of lamellae.

Fig. 1 shows a theoretical $g_1(r)$ function for distance statistics resulting from independent variations σ_1 and σ_2 of the thickness d_1 and d_2 of the lamellae of phases 1 and 2, respectively, within a given stack. The solid line is computed for infinite stack size, the broken line for an average of six lamellae of each kind per stack.

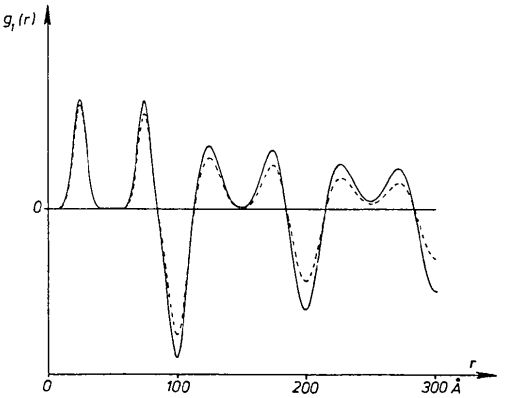

Fig. 1. Theoretical interface distribution $g_1(r)$ for a stacking statistics. $v_c=0{\cdot}75$, $L=100$ Å, $\sigma_a=\sigma_c=5$ Å, solid line $t=\infty$, broken line $t=600$ Å.

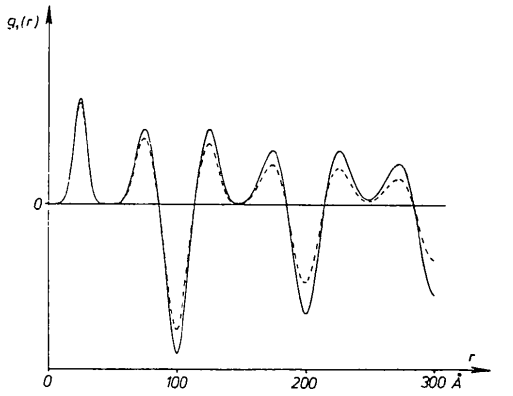

Fig. 2. Theoretical interface distribution $g_1(r)$ for a lattice statistics. $v_c=0{\cdot}75$, $L=100$ Å, $\sigma_a=\sigma_L=5$ Å, solid line $t=\infty$, broken line $t=600$ Å.

In this case, the change of σ_i with i is given by the relationships

$$\sigma_i^2 = n(\sigma_1^2+\sigma_2^2) \quad \text{for} \quad i=3n,$$
$$\sigma_i^2 = n(\sigma_1^2+\sigma_2^2)+\sigma_1^2 \quad \text{for} \quad i=3n+1,$$
$$\sigma_i^2 = n(\sigma_1^2+\sigma_2^2)+\sigma_2^2 \quad \text{for} \quad i=3n+2.$$

Fig. 2 shows a theoretical $g_1(r)$ function for distance statistics resulting from an independent variation of the thickness d_1 and the spacing L between the centers of the lamellae of the same phase within a given stack, for finite and infinite stack size. In this case, the change of σ_i with i is given by the relationship

$$\sigma_i^2 = n(\sigma_1^2/2+\sigma_L^2) \quad \text{for} \quad i=3n \quad \text{and} \quad i=3n\pm1.$$

Fig. 3 shows a theoretical $g_1(r)$ function for distance statistics resulting from a variation of the parameters of the lamellar structure from one stack to another, assuming the structure within each individual stack to be perfectly periodic and containing the same volume fractions of the two phases. In this case the distance distributions h_i expand linearly with r_i so that the ratio σ_i/r_i is constant.

An inspection of these three figures reveals that the $g_1(r)$ functions are, apparently, rather insensitive to changes of the stack size. This is due to the fact that the stack size has only little effect on $g_1(r)$ at relatively small values of r, and that the values of $g_1(r)$ at larger r values, where the effect of finite stack size would be more pronounced, are heavily affected by the overlap of adjacent distance distributions with opposite sign.

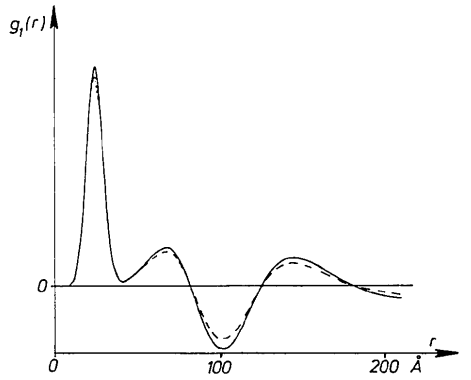

Fig. 3. Theoretical interface distribution $g_1(r)$ for a homogenous L distribution. $v_c=0{\cdot}75$, $L=100$ Å, $\sigma_a=5$ Å, solid line $t=\infty$, broken line $t=600$ Å.

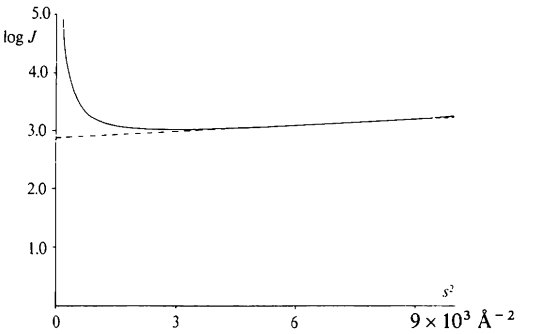

Fig. 4. Determination of the fluctuation component by a log Js^2 plot (sample 2).

This observation suggests that the information obtainable on the stack size depends strongly on the type of the distance statistics present, and that the values for the stack size determined by a fitting of theoretical scattering curves to experimental ones may be affected by large errors if the approximation chosen for the distance statistics is not correct.

3. Experimental

Five samples of commercial polyethylene were chosen for the experiments:

1. Lupolen 1800 H (BASF), a branched polyethylene with a crystallinity of 39% (36 branches per 1000 monomer units).
2. Lupolen 4261 Z (BASF), a linear polyethylene with a crystallinity of 58%.
3. Lupolen 5041 D (BASF), a branched polyethylene with a crystallinity of 65% (9 branches per 1000 monomer units).
4. Lupolen 6041 D (BASF), a linear polyethylene with a crystallinity of 74%.
5. The same starting material as sample 4 with a crystallinity of 83% obtained by annealing at 135 °C for one week.

The crystallinity of these samples was determined by X-ray wide-angle scattering, calorimetry and density methods. The results of these methods differ only by a few percent. The small-angle scattering was measured with a Kratky camera using Cu $K\alpha$ radiation, a graphite monochromator, a Xenon-filled proportional counter and pulse-height discrimination.

In order to obtain a high accuracy, especially at larger s values, the scattering curves were measured with different vertical slit dimensions in three overlapping angular regions. After correcting for the finite vertical slit dimensions using a modified version of Vonk's (1971) program, these curves were fitted together. Fig. 4 shows a log J *vs* s^2 plot of such a curve in which the fluctuation component J_{Fl} is determined by an extrapolation from larger s values. The function $s^3(J-J_{Fl})$ is then plotted against s^2 in order to detect the region in which Porod's law is valid. Fig. 5 shows such a plot from which l_p, the Porod parameter (as defined by Ruland, 1977), and d_z, the average thickness of the domain boundary, are obtained. If d_z is known, the scattering curve can be corrected for the finite width of the domain boundary, which results in the determination of J_{id}. From the latter the correct value for Porod's invariant k (for the determina-

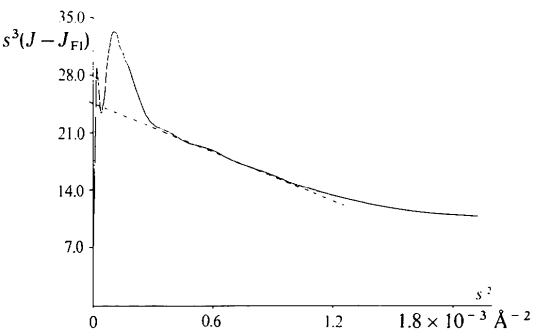

Fig. 5. Determination of the thickness of the domain boundary (sample 2).

tion of l_p) can be obtained with the expression

$$k = 2\pi \int_0^{s_{Max}} sJ_{id}(s)ds + \frac{2\pi}{s_{Max}} [\lim_{s\to\infty} s^3 J_{id}(s)],$$

in which the second term on the right-hand side represents an estimate of the integral within the limits s_{Max} to infinity. With equation (3) the interference function $\tilde{G}_1(s)$ is obtained from J_{id} and its Fourier Bessel transform defined by equation (4) results in the determination of the interface distribution function $g_1(r)$. Fig. 6 shows an example of $\tilde{G}_1(s)$ and Fig. 7 the corresponding $g_1(r)$.

In order to check the direct computation of $g_1(r)$ from $G_1(s)$, we have carried out a complete desmearing of the experimental scattering curve using the computer program of Vonk (1971). Fig. 8 shows the interference function $G_1(s)$, as defined by equation (1), corresponding to the $G_1(s)$ function shown in Fig. 6, and Fig. 9 shows $g_1(r)$ obtained from $G_1(s)$ by Fourier cosine transform. A comparison of these curves reveals that both ways of computing $g_1(r)$ lead to essentially the same result, but the direct computation from $G_1(r)$ is, of course, preferable since it minimizes computation time and errors.

The curves shown in Figs. 7 and 9 correspond to earlier measurements of sample 2 and are given only to demonstrate the equivalence of the two ways of computation. For the final evaluation of $g_1(r)$, an improved measurement of $\tilde{G}_1(s)$ has been used and the values given in Table 2 for sample 2 do thus not correspond to the evaluation of Fig. 7 or Fig. 9.

4. Results and discussion

The structural parameters obtained from the evaluation of $J_{obs}(s)$ and $g_1(r)$ are in Table 2. The evaluation of $g_1(r)$ was carried out with a DuPont curve analyzer.

Table 2. *Structural parameters obtained from the evaluation of J_{obs} and g_1*

Sample	d_z (Å)	l_p (Å)	$\bar{d}_a$ (Å)	σ_a (Å)	$\bar{d}_c$ (Å)	L (Å)
1	11	48	40	18	50	90
2	9	76	32	15	148	180
3	10	68	30	13	143	173
4	8	82	38	18	239	277
5	<3	93	40	19	308	348

The thickness of domain boundary d_z is about 10 Å for all samples except the highly annealed one with a tendency of the branched polyethylene to have somewhat higher values than the linear ones. The latter effect has already been observed by Vonk (1973). The average thickness of the amorphous lamellae and its r.m.s. variation are about the same for all samples; the differences in the long period L are mainly due to the differences in the average thickness $\bar{d}_c$ of the crystalline lamellae. The r.m.s. variation of L and $\bar{d}_c$ cannot be determined unambiguously, since the corresponding distributions show in all cases a strong overlap. In the case of samples 3, 4 and 5, there are indications of a bimodal distribution of $\bar{d}_c$ and L which could be attributed to the formation of superstructures with different L values at different stages of the crystallization process. Interface distances of higher order cannot be resolved with sufficient accuracy to derive quantitative information of the type of stacking statistics, as discussed in the theoretical section. However, the general aspect of the $g_1(r)$ functions obtained resembles strongly that of the

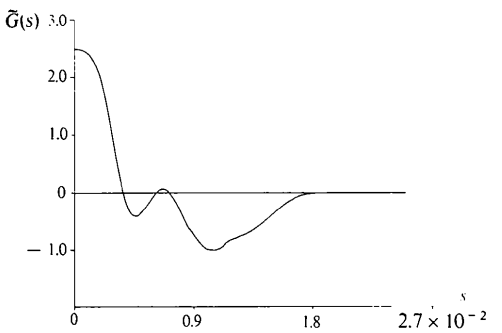

Fig. 6. The interference function $\tilde{G}_1(s)$ obtained from the slit-smeared scattering curve of sample 2.

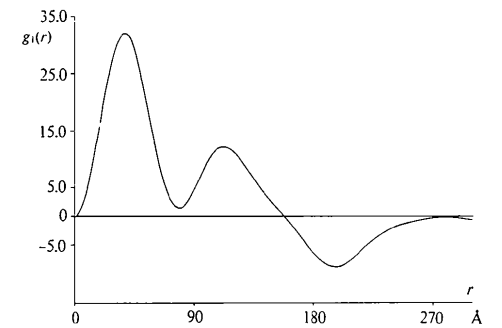

Fig. 7. The interface distribution function $g_1(r)$ obtained from $\tilde{G}_1(s)$ (sample 2) by Fourier–Bessel transformation.

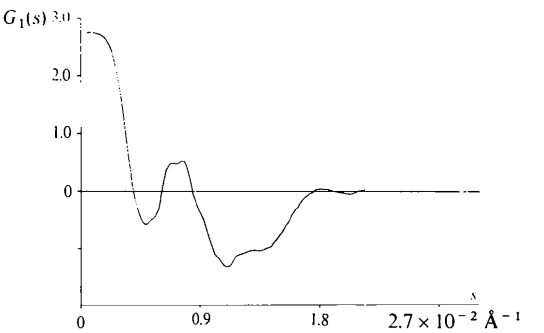

Fig. 8. The interference function $G_1(s)$ obtained from the desmeared scattering curve of sample 2.

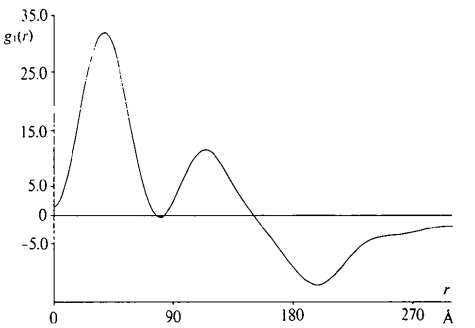

Fig. 9. The interface distribution function $g_1(r)$ obtained from $G_1(s)$ (sample 2) by Fourier cosine transformation.

$g_1(r)$ functions calculated for homogeneous L distributions (see Figs. 3, 7 and 9), the other types of stacking statistics could only be fitted to the observed $g_1(r)$ curves if unreasonably small stack sizes (average numbers of layers per stack smaller than two) were considered.

It can be expected that the information obtainable from interface distribution functions is limited to smaller distances in a similar way and for similar reasons, as radial atomic distributions functions give unambiguous information only on the shorter interatomic distances. Further information can possibly be obtained by taking the basic parameters determined from the $g_1(r)$ functions and computing theoretical $G_1(s)$ or $\tilde{G}_1(s)$ functions for which supplementary parameters are chosen by a least-squares fitting to the experimental $G_1(s)$ or $\tilde{G}_1(s)$ functions. A starting point could be the Fourier cosine transform of equation (5),

$$G_1(s)=\sum_{i=1} w_i H_i(s)\cos 2\pi r_i s, \tag{6}$$

where $H_i(s)=\exp(-2\pi^2\sigma_i^2 s^2)$. From the experimental $g_1(r)$ functions a good first approximation for the r_i values and for some w_i and σ_i values of lower i could be deduced, the higher-order ones are then determined by trial and error. Since $\tilde{G}_1(s)$ is related to $G_1(s)$ by

$$G_1(s)=2s^3\int_0^\infty \frac{G_1[(s^2+y^2)^{1/2}]}{(s^2+y^2)^2}\,\mathrm{d}y \tag{7}$$

and since the terms corresponding to $H_i(s)\cos 2\pi r_i s$ in a series development of $\tilde{G}_1(s)$ are not obtainable in a closed form, the most practical way for a trial-and-error method for $\tilde{G}_1(s)$ functions is probably the computation of $G_1(s)$ according to equation (6) and a subsequent conversion to $\tilde{G}_1(s)$ using equation (7).

While these possibilities have to be tested in further studies, there is already some interesting information obtainable from the data given in Table 2. First of all, the ratio $\bar{d}_c/L$ gives the volume fraction of crystalline domains within the stacks of lamellae, a parameter which is often referred to as the 'linear' crystallinity. In contrast to other methods, *e.g.* that of Tsvankin, Zubov & Kitaigorodskii (1968), this value of linear crystallinity does not depend on the validity of the structural model chosen for the evaluation. A comparison with the bulk crystallinity obtained by other methods (wide-angle X-ray diffraction, calorimetry, density) shows that the values for the linear crystallinity are always equal to or larger than those of the bulk crystallinity, which suggests that the difference between the two values is due to the presence of amorphous domains which are not part of the lamellar structures. The ratio of the bulk crystallinity to the linear crystallinity is, accordingly, the volume fraction v_l of lamellar structures. These values are shown in the first column of Table 3. An inspection of these values reveals that the volume fraction of lamellar structures is increasing with increasing crystallinity and that these structures occupy nearly the total volume only in the sample of the highest crystallinity.

Table 3. *Volume fractions of various types of domains*

Sample	v_l	v_z	v_c	v_{ai}	v_{aa}	v_c'
1	0·70	0·18	0·30	0·22	0·30	0·39
2	0·71	0·07	0·55	0·09	0·29	0·58
3	0·79	0·09	0·61	0·09	0·21	0·65
4	0·86	0·05	0·72	0·09	0·14	0·74
5	0·94	<0·01	0·83	0·11	0·06	0·83

The existence of a finite thickness of the domain boundaries poses the question of the volume occupied by these boundaries. To a first approximation the fraction v_z of the total volume occupied by these boundaries is

$$v_z=\frac{2d_z v_l}{L}.$$

The values obtained are listed in the second column of Table 3; they show that v_z is not negligibly small except for the sample with the highest crystallinity. If the values for v_l and v_z are considered, it is obvious that a complete balance of volume fractions involves the description of the structure in terms of a four-component system: crystalline domains (volume fraction v_c), amorphous domains inside the lamellar structures (v_{ai}), amorphous domains outside the lamellar structures (v_{aa}) and domain boundaries (v_z). Since the domain boundaries are predominantly within the lamellar structures, half of the value of v_z has to be subtracted from the volume fraction v_c' of crystalline domains as determined on the basis a two-component approximation, *e.g.* wide-angle X-ray scattering, calorimetry, density, and the other half from the volume fraction of the amorphous domains inside the lamellar structure. Hence

$$v_c=v_c'-v_z/2$$
$$v_{ai}=v_l-v_c-v_z$$
$$v_{aa}=1-v_l\,.$$

The values obtained for these volume fractions together with the values of v_c' are listed in columns 3 to 6 of Table 3. Except for sample 1, the values of v_c are only a few percent lower than those of v_c', a difference which could be considered as still within the limits of error of a crystallinity determination. Of more interest is the observation that, except for sample 1, the values of v_{ai} are about the same for the rest of the samples and that the increase of v_c is mainly due to a decrease of v_{aa}, which means an increase of v_l.

On account of the small number of samples studied it does not seem appropriate to discuss the results any further. The work has shown the potential of a more detailed analysis of the small-angle scattering data. An application of this method to a larger number of samples with a well defined history can be expected to increase our knowledge about the change of the lamellar structure as a function of various parameters determining the crystallization behaviour of polymers.

The authors are indebted to the Deutsche Forschungsgemeinschaft for sponsoring this research project.

References

BRÄMER, R. (1974). *Colloid Polym. Sci.* **252**, 504–515.

KILIAN, H. G. & WENIG, W. (1974). *J. Macromol. Sci. Phys.* **9**, 463–482.

RATHJE, J. & RULAND, W. (1976). *Colloid. Polym. Sci.* **254**, 358–370.

RULAND, W. (1974). *J. Appl. Cryst.* **7**, 383–386.

RULAND, W. (1977). *Colloid. Polym. Sci.* **255**, 417–427.

STROBL, G. R. & MÜLLER, N. (1973). *J. Polym. Sci. Polym. Phys. Ed.* **11**, 1219–1233.

TSVANKIN, D. YA., ZUBOV, YU. A. & KITAIGORODSKII, A. I. (1968). *J. Polym. Sci. Part* C16, 4081–4091.

VONK, C. G. (1971). *J. Appl. Cryst.* **4**, 340–342.

VONK, C. G. (1973). *J. Appl. Cryst.* **6**, 81–86.

VONK, C. G. & KORTLEVE, G. (1967). *Kolloid-Z. Z. Polym.* **220**, 19–24.